Depletion interaction between spheres immersed in a solution of ideal polymer chains

Remco Tuinier[a)]
Van't Hoff Laboratory, Debye Research Institute, University of Utrecht, Padualaan 8, 3584 CH Utrecht, The Netherlands

Gerrit A. Vliegenthart
School of Chemistry, University of Bristol, Cantock's Close, Bristol, BS8 1TS United Kingdom

Henk N. W. Lekkerkerker
Van't Hoff Laboratory, Debye Research Institute, University of Utrecht, Padualaan 8, 3584 CH Utrecht, The Netherlands

(Received 28 June 2000; accepted 19 September 2000)

The depletion interaction between two spheres due to nonadsorbing ideal polymers is calculated from the polymer concentration profile using the excess (negative) adsorption. Computer simulations show that the polymer concentration profiles around two spheres are well described by the product function of the concentration profile around a single sphere. From the interaction potential between two spheres the second osmotic virial coefficient, B_2, is calculated for various polymer-colloid size ratios. We find that when the polymers become smaller than the spheres, B_2 remains positive in the dilute regime. This shows that the depletion interaction is ineffective for relatively small spheres. © *2000 American Institute of Physics.* [S0021-9606(00)50247-5]

I. INTRODUCTION

The polymer-induced depletion interaction between colloidal particles has been studied extensively during the last decades.[1–9] The pioneering work on depletion interaction between particles due to nonadsorbing polymers was done by Asakura and Oosawa,[1] and further elaborated by Vrij,[2] and Joanny *et al.*[3] Subsequently, their concepts were verified experimentally by Vincent and co-workers,[4,5] and De Hek and Vrij.[6] Since the early eighties, depletion interaction theories of mixtures of spheres and polymer chains were extended in the sense that complete phase diagrams can be calculated within a perturbation framework.[7,8] The topology of the phase diagrams, which only depends on the ratio R_g/R, where R is the colloid radius and R_g is the radius of gyration, is qualitatively described very well by these theories, and is supported by computer simulations.[10,11] More recently the theoretical work has been extended, taking into account polydispersity.[12–14] Most of these theoretical approaches[2,7,8,12–14] replace the polymer chains by penetrable hard spheres (PHS) in order to simplify the polymer chains and take the radius of gyration of the polymers as the radius of the PHS.

Milling and Biggs[15] found quantitative agreement between the depletion force predicted theoretically and the force measured between a silica plate and a silica sphere immersed in a cyclohexane solution of PDMS for $R/R_g \approx 400$. They showed that the range of the interaction potential is very close to $2R_g$, which corroborates that the depletion layer thickness is close to the radius of gyration for relatively very small polymer chains. For experiments on systems with polymers that are much smaller than the colloidal spheres (the ''colloid limit''), the PHS treatment works out well.[16] However, we also compared these PHS theories to experiments where the colloid radius is of the order of the polymer radius of gyration,[17–20] and found that the theoretical curves lie far below the experimental ones.

If the polymers become much larger than the colloids, the PHS approach is known to fail.[21–28] In that limit, also referred to as the ''protein limit,'' the colloids can penetrate the polymer coil and a proper description of the system becomes complicated, since the spatial structures of polymer chains have to be taken into account properly. De Gennes[21] showed that dispersing small spheres in a semidilute polymer solution does not lead to a phase separation. Following De Gennes, a range of studies was done to describe the stability of colloid–polymer solutions in the protein limit.[22–28] These studies are relevant, for instance, for the stability of food products where proteins, which can be regarded as spheres if globular, and polysaccharides are often mixed, giving rise to depletion-induced phase separations.[29–32]

In this paper we study the interaction between two spheres immersed in an ideal polymer solution of long chains for arbitrary polymer–colloid size ratios. As a tool we use the adsorption method,[33–35] which uses the polymer concentration profiles to calculate the (negative) adsorption, and hence the interaction between colloidal particles. Our method uses a superposition approximation resulting in a product function that describes the polymer concentration profile between two plates or two spheres. We will use the interaction between two plates (Sec. II), calculated exactly using the force method, as a reference case to test our method. It will be shown that the interaction between two plates calculated using the force method is in quantitative

a)Author to whom correspondence should be addressed. Electronic mail: r.tuinier@chem.uu.nl

agreement with that of a negative adsorption method using the product of the polymer concentration profiles. Further, the polymer concentration profiles were tested using computer simulations. In Sec. III, we will apply the (negative) adsorption method to the case of two spheres and calculate the second osmotic virial coefficient of two spheres as a function of the polymer concentration for various polymer–colloid size ratios. Above a certain polymer–colloid size ratio, we find that the depletion interaction is too weak to cause phase separation and thus the colloid–polymer mixtures are stable.

II. INTERACTIONS BETWEEN TWO FLAT PLATES IMMERSED IN SOLUTION OF IDEAL POLYMER CHAINS

A. Interaction potential between two flat plates using the force method

The force per unit area between two parallel flat plates, $K(h)$, is the difference between the osmotic pressure between (inside) the plates Π_i, and outside the plates, $\Pi_o = kTn_b$, where n_b is the bulk number density of polymers, and reads[1]

$$K(h)=n_b kT\left(X(h)-1+h\frac{\partial X(h)}{\partial h}\right), \tag{1}$$

where $X(h)$ is defined as

$$X(h)=\frac{8}{\pi^2}\sum_{p=1,3,5,\ldots}\frac{1}{p^2}\exp\left(-\frac{p^2\pi^2R_g^2}{h^2}\right), \tag{2}$$

where the radius of gyration of ideal chains is defined as $l\sqrt{(N/6)}$, where l is the segment size, and N is the number of links between the segments. Integration of this force yields the interaction potential per unit area between the plates $W(h)$

$$\frac{W(h)}{kT}=-n_b\left(X(h)h-h+\frac{4R_g}{\sqrt{\pi}}\right). \tag{3}$$

For penetrable hard spheres, Vrij[2] found

$$\frac{W_{\mathrm{PHS}}(h)}{kT}=-n_b(\sigma_{\mathrm{PHS}}-h), \tag{4}$$

where σ_{PHS} is the diameter of a penetrable hard sphere. For $h=0$ we find from Eqs. (3) and (4) that σ_{PHS} is equal to $4R_g/\sqrt{\pi}$ if we match the minima of the potentials. Both the predictions of Eqs. (3) and (4) are plotted in Fig. 1, and the agreement is very good for $h<3R_g/2$. For $h>2R_g$ the interaction potentials deviate strongly; ideal polymer chains have a longer range of attraction than the penetrable hard spheres. Eisenriegler[36] noted that Eq. (3) is identical to Eq. (4) up to and including terms of the order of h^4. PHS are thus very good replacements for ideal chains to describe the interactions for flat walls, and hence are equally expected to behave very well for very large spheres.

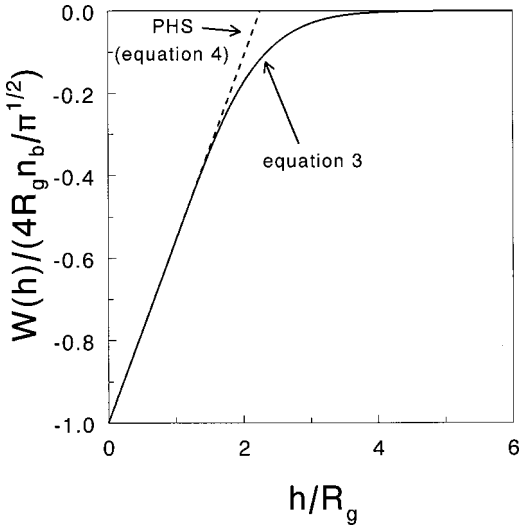

FIG. 1. Normalized interaction potential between two hard plates immersed in an ideal polymer solution as a function of the normalized distance between the plates h/R_g. The predictions for ideal polymer chains [Eq. (3)] is given by the solid curve and that of penetrable hard spheres [PHS; Eq. (4)] is given by the dashed curve.

B. Interaction potential between two plates using the adsorption method

An alternative way to obtain the interaction potential is by making use of the generalized Gibbs equation (see, for instance, Refs. 33–35, 37)

$$-\left(\frac{\partial W(h)}{\partial\mu}\right)_h=\Gamma(h)-\Gamma(\infty), \tag{5}$$

where μ is the chemical potential of the polymer solution, and $\Gamma(h)$ is the adsorbed amount of polymers per unit area, i.e., the number of polymer chains between the plates per unit area when the distance between the plates equals h. The adsorption is the integral over the polymer concentration profile $n(x)$

$$\Gamma(h)=\int_0^h dx[n(x)-n_b]. \tag{6}$$

Since for ideal chains $\mu=kT\ln(n_b)$, and $[\Gamma(h)-\Gamma(\infty)] \sim n_b$, Eq. (6) yields

$$W(h)=-kT[\Gamma(h)-\Gamma(\infty)]. \tag{7}$$

Thus, the profile of the polymer concentration between the two plates yields the interaction potential. If the two plates touch, the negative adsorption is zero $[\Gamma(0)=0]$, and $W(0)=kT\Gamma(\infty)$. From Eq. (3) we find $W(0) =-kTn_b4R_g/\sqrt{\pi}$, which says that $\Gamma(\infty)=-n_b4R_g/\sqrt{\pi} =-2n_b\xi$, where ξ is the depletion layer thickness per plate, which thus equals $2R_g/\sqrt{\pi}$. We find from Eqs. (7) and (3) for $\Gamma(h)$

$$\Gamma(h)=n_b(X(h)h-h). \tag{8}$$

In order to calculate the polymer concentration profile between two flat plates $n(x)$, we first focus on the polymer concentration profile near a single plate. Analytical expressions for a polymer in solution near an interface can be ob-

tained using an analogy between a Brownian diffusion process and the path of subsequent segments in a polymer chain, using proper boundary conditions. The relation describing the resulting probability function of a polymer chain is termed Edwards' diffusion equation.[38–41] Eisenriegler,[42] and later Marques and Joanny,[43] calculated the polymer concentration near one flat plate for ideal chains, and found the following expression for the relative polymer concentration $f(x)=n(x)/n_b$:

$$f(x)=\frac{n(x)}{n_b}=2\,\mathrm{erf}(z)-\mathrm{erf}(2z)+\frac{4z}{\sqrt{\pi}}[\exp(-z^2)-\exp(-4z^2)]+8z^2\left[\frac{1}{2}-\mathrm{erf}(2z)+\frac{1}{2}\mathrm{erf}(z)\right], \quad (9)$$

where z is defined as $x/(2R_g)$, and x is the distance from the surface. One can characterize the negative adsorption by the depletion layer thickness, ξ, defined as

$$\xi=\int_0^\infty dx\left(1-\frac{n(x)}{n_b}\right). \quad (10)$$

For the case of ideal polymer chains near a flat plate [Eq. (9)] we find a depletion layer thickness, ξ, equal to $2R_g/\sqrt{\pi}$, which is in agreement with the analysis above Eq. (8). We note here that the simple form $n(x)/n_b=\tanh^2(x/\xi)$, derived by De Gennes[39] in the context of depletion of polymer segments in a semidilute polymer solution in a good solvent, describes Eq. (9) within an accuracy of 1%.

In order to be able to describe the interaction between spheres later on, we propose the following product function:

$$\frac{n(x)}{n_b}=f(x)f(h-x), \quad (11)$$

to make a connection between the individual profile of the nonadsorbing ideal polymers near a single plate and the profile between two plates. In Eq. (11) $n(x)$ is the polymer concentration between the plates, and $f(x)$ and $f(h-x)$ are the individual profiles, given by Eq. (9). The concentration profile near a single plate, say plate 1, can be expressed by a Boltzmann factor as: $f(x)=n(x)/n_b=\exp[-V(x)/kT]$, where $V(x)$ is the free energy giving rise to the profile. For the second plate, located at a distance h, we can then write: $f(h-x)=n(h-x)/n_b=\exp[-V(h-x)/kT]$. Subsequently, the product function Eq. (11) follows from the superposition approximation: $V_{\mathrm{tot}}(x)=V(x)+V(h-x)$.

In order to test Eq. (11) we compare its results with computer simulations, as plotted in Fig. 2. The computer simulations (symbols) were obtained by placing random walks of 100 segments in a box containing two flat plates. All configurations are weighted with equal probability, but those crossing the plates are assigned a zero weight. The computer simulation setup is consistent with that of Feigin and Napper.[44] It follows from the results in Fig. 2 that the product function [Eq. (11); full curves] gives a good description of the computer simulations for $h/R_g>3$. For $h/R_g<\pi$, the sum of $X(h)$ of Eq. (2) is dominated by $p=1$. Then, one can use a ground-state approximation to Edwards' diffusion equation to calculate the polymer concentration profile for small gap widths. For that situation the largest eigenvalue dominates in the expansion and the profile is then described as[39–41]

$$\frac{n(x)}{n_b}=\frac{16}{\pi^2}\exp\left(-\frac{\pi^2R_g^2}{h^2}\right)\sin^2\left(\frac{\pi x}{h}\right). \quad (12)$$

So, for small gap widths we can compare the product function with the results of Eq. (12). In Fig. 2 we have plotted both the predictions of Eq. (11) (solid curves) as well as those of Eq. (12) for $h/R_g=2$, and 1.5 (dashed curves). Obviously, Eq. (11) overestimates the ground-state Eq. (12). Thus, the relative deviation is large for small plate separations, which agrees with the expectation that the superposition approximation could be deficient for very small plate separations. However, the absolute deviation for the interac-

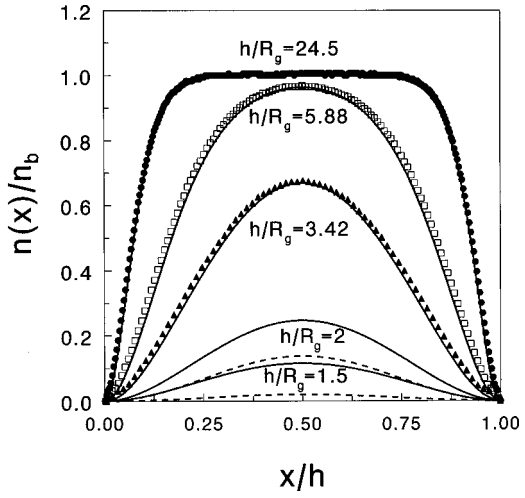

FIG. 2. Polymer concentration profiles between two flat plates. The symbols correspond to the computer simulations for 100 segments. The full curves are the predictions according to the product function Eq. (11) [using Eq. (9)], and the dashed curves are the ground-state approximation results using Eq. (12).

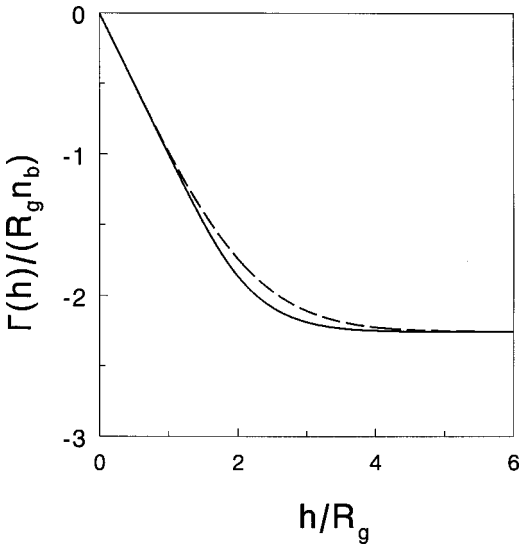

FIG. 3. Normalized adsorbed amount $\Gamma(h)$ as a function of the normalized plate separation h/R_g, using the exact result [solid curve; Eq. (8)], and from the product function for the profile [Eqs. (6), (9), and (11)].

tion is small; the distance between the plates becomes small and therefore $\Gamma(h)/\Gamma(\infty)\rightarrow 0$ for small h [see Eq. (6)].

In order to test whether the product function [Eq. (11)] yields a good prediction of the adsorption $\Gamma(h)$, we compared it with the exact result of Eq. (8) in Fig. 3. The exact result is plotted as the solid curve and the adsorption, using the product function as calculated from inserting Eq. (11) into Eq. (6) is plotted as the dashed curve in Fig. 3. The results are generally consistent but differ somewhat for intermediate plate separations. We conclude here that Eq. (11) is a function that describes the main features of the polymer concentration profile, and hence the resulting adsorption and interaction between two flat plates. It follows that the calculation of the depletion layer thickness for a single plate suffices to describe the depletion interaction between two plates. We therefore assume that the depletion layer that follows from the polymer concentration profile near a single sphere can also be used to describe the interactions between two spheres. First, we will focus on the polymer concentration profile near a single sphere.

III. SPHERES IMMERSED IN AN IDEAL POLYMER CHAIN SOLUTION

A. Ideal polymer chains near a single sphere

Taniguchi *et al.*,[45] and independently Eisenriegler *et al.*,[22] found the concentration of ideal polymer chains around a single hard sphere with radius R which reads

$$f(x)=\left(\frac{R}{R+2zR_g}\right)^2\left[\begin{array}{l}\left(\frac{2zR_g}{R}\right)^2+\left(\frac{zR_g}{R}\right)\left(\mathrm{erf}(z)-2z^2(1-\mathrm{erf}(z))+\frac{2}{\sqrt{\pi}}z\exp(-z^2)\right)\\ +2\,\mathrm{erf}(z)-\mathrm{erf}(2z)+\frac{4z}{\sqrt{\pi}}[\exp(-z^2)-\exp(-4z^2)]\\ +8z^2\left[\frac{1}{2}-\mathrm{erf}(2z)+\frac{1}{2}\mathrm{erf}(z)\right]\end{array}\right], \tag{13}$$

where z again equals $x/2R_g$, and where x is the distance from the surface of the sphere. We first note that Eq. (13) approaches Eq. (9) in the limit $R\gg R_g$. In the limit of very small particle radii, we arrive at the limit $n(x)/n_b=(x/\{R+x\})^2=(1-R/\{R+x\})^2$. A similar limit was also found by Odijk[25] for a small colloidal sphere immersed in a semidilute polymer solution with a correlation length being much larger than the colloid radius. In the ''protein'' limit where $R_g\gg R$, the profile becomes independent of the relevant polymer length scale.

For various ratios of R_g/R we plotted the profiles as a function of the distance from the interface in Fig. 4 as the dashed curves, as well as the single plate result (solid curve) of Eq. (9). In Fig. 4 we also added computer simulation data (symbols). The simulations were obtained by placing random walks in a box containing a single flat plate or a single sphere. We observe that the simulation results are in agreement with Eqs. (9) and (13). For large radii ($R_g/R=0.1$) we

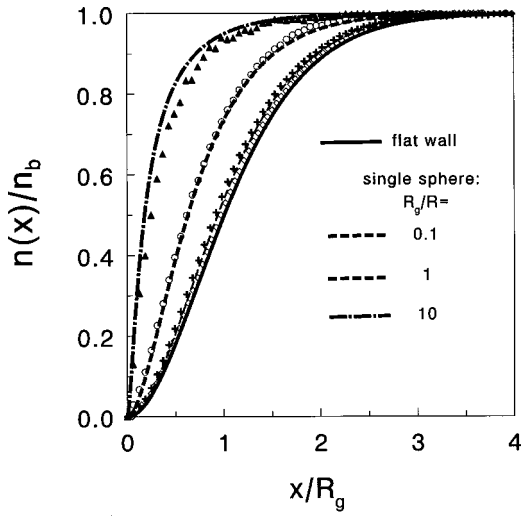

FIG. 4. Polymer depletion layer profiles for ideal nonadsorbing polymer chains near a flat plate [solid curve; Eq. (9)] and near a sphere [dashed curves; Eq. (13)] as a function of the distance from the surface x. The results of the computer simulations are given for the flat plate (open diamonds), and the single sphere for $R/R_g=0.1$ (crosses), 1 (open circles), and 10 (closed squares).

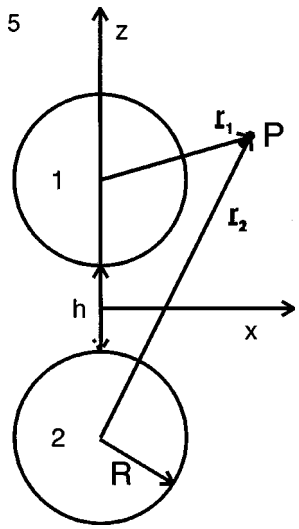

FIG. 5. Schematic picture of the geometry of two spheres separated by a distance h. The relevant parameters are indicated in the figure.

see that the sphere profile approaches that of a flat plate [Eq. (9)]. For $R_g/R=1$ the depletion layer thickness already becomes significantly smaller than $2R_g/\sqrt{\pi}$. For very small spheres ($R_g/R=10$), the depletion layer is of the order of the sphere radius, rather than of the order of the radius of gyration. For $R_g \gg R$ we find a limiting value of $\xi \approx 3R$.

B. Interaction between two spheres immersed in a solution with ideal polymers

In Sec. II we showed that the product function [Eq. (11)] describes the interactions between two flat plates quite well in comparison with exact expressions for the interaction potential of two plates. Here, we apply the product function to calculate the interactions between spherical colloids immersed in a polymer solution. First, we calculate the polymer concentration profile in the space surrounding two spheres immersed in an ideal polymer solution. A schematic two-dimensional picture of the situation is given in Fig. 5 for two spheres with a center-to-center distance of $h+2R$. We assume that the local polymer concentration $n_s(r)$ in every point defined by the vector r is given by a product function

$$\frac{n_s(r)}{n_b} = f_s(r_1) f_s(r_2), \tag{14}$$

where $f_s(r_i)$ is the polymer concentration profile given by Eq. (13), and r_i is the closest distance to the surface of sphere i. Several computer simulation results (symbols) for $R/R_g=10$ are plotted in Figs. 6(a)–6(d) as a function of z (normalized by R_g) and are compared with the result of the product function given by Eq. (14). In Fig. 6(a) we focus on the profiles along sphere 1 while sphere 2 touches it ($h=0$). For $h/R_g=0.77$, 3.1, and 7 we present the concentration profiles between the spheres in Figs. 6(b)–(d) for various values of x (normalized by R_g). For the situation where the spheres have a comparable size as the polymer chains ($R/R_g=1.4$), we also present computer simulation results (symbols) for $h/R_g=0.77$, and 3.1 in Figs. 7(a) and (b), respectively. In general, we observe that the profiles are in fair agreement with the predictions of the product function.

In order to arrive at the interactions between the spheres, we calculate the (negative) adsorption around two colloidal spheres immersed in a polymer solution using the product

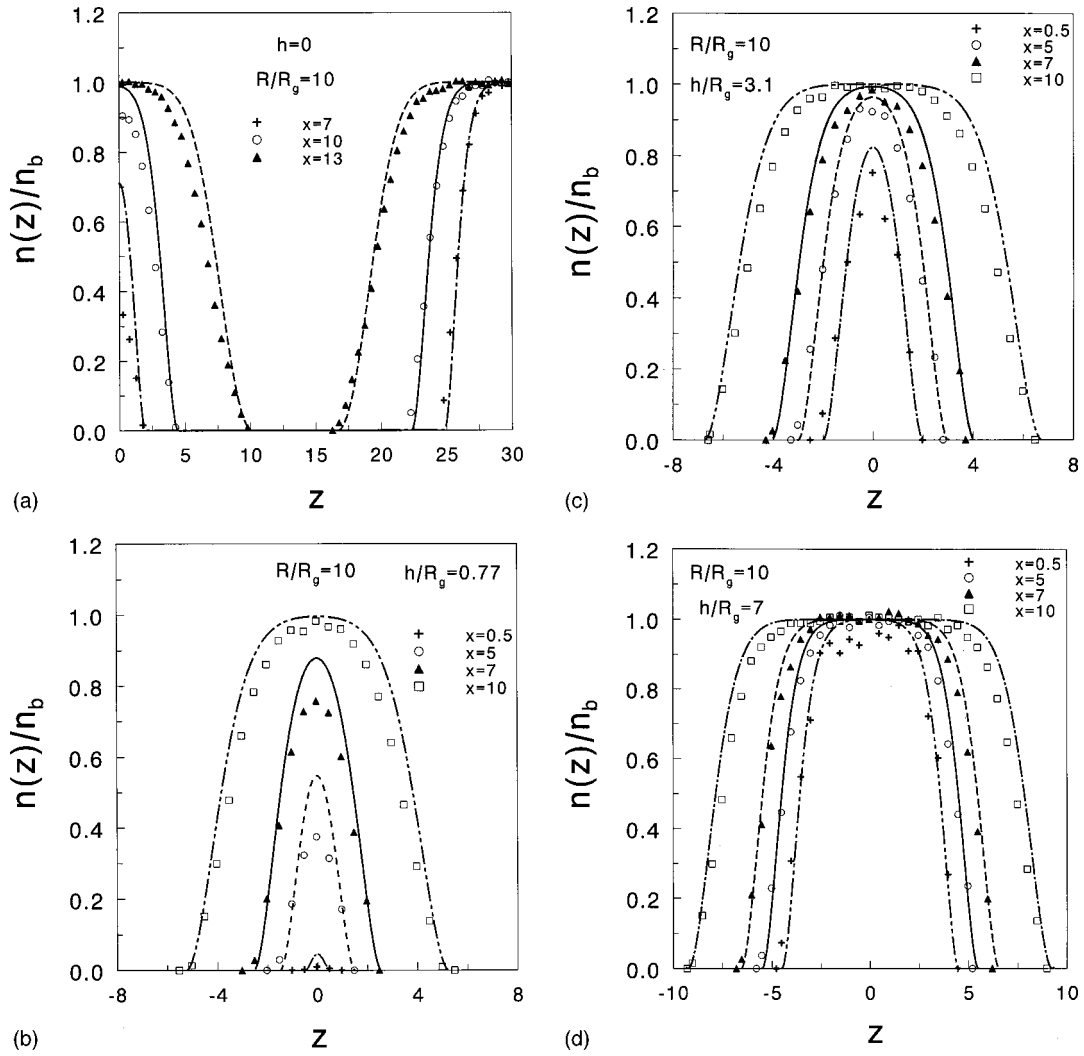

FIG. 6. (a) Polymer concentration profiles in the region around two spheres for $R/R_g=10$, $h=0$ and $x=7$, 10, and 13. The symbols are the results from the computer simulations. The curves correspond to the result of the product function expressed by Eq. (14). (b) As (a) for $h/R_g=0.77$, and $x=0.5$, 5, 7, and 10. (c) As (a) for $h/R_g=3.1$. (d) As (a) for $h/R_g=7$.

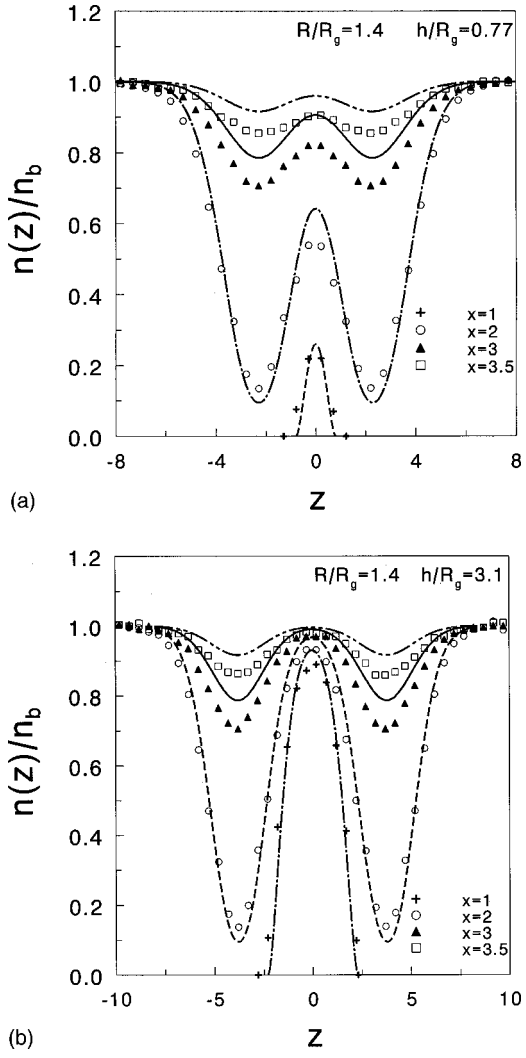

FIG. 7. (a) Polymer concentration profiles for $R/R_g=1.4$ in the region around two spheres for $h/R_g=0.77$ and $x=1$, 2, 3, and 3.5. The symbols are the results from the computer simulations. The curves correspond to the result of the product function expressed by Eq. (14). (b) As (a) for $h/R_g=3.1$.

function to describe the profiles around the particles. The negative adsorption is now the excess number of polymers per volume and is denoted as $N(h)$, where h is the closest sphere-to-sphere distance. From the (negative) adsorption we can calculate the interaction potential from Eq. (8). It follows that the interaction potential between two spheres, $W_s(h)$, is related to $N(h)$ as

$$\frac{W_s(h)}{kT}=N(\infty)-N(h). \tag{15}$$

The result for $R/R_g=100$ is plotted in Fig. 8 (dashed curve). We normalized the interaction potential curves by dividing over the absolute value of the minimum of the curves. In this large sphere limit we can apply the Derjaguin approximation[46] to the result of the force method [Eq. (4)]

$$W_s(h)=\int_h^\infty dh'\ \pi R W(h'), \tag{16}$$

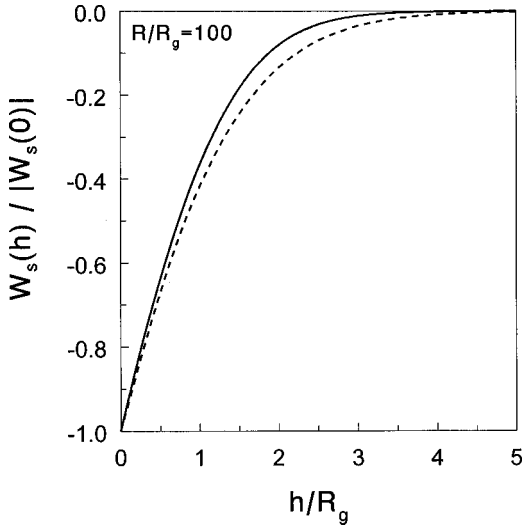

FIG. 8. Interaction potential between two spheres immersed in an ideal polymer solution normalized by the depth of the minimum for $R/R_g=100$. The dashed curve is the result from the adsorption method [Eq. (15)] using the product function [Eqs. (14)]. The solid curve is the result of the Derjaguin approximation to the result of the force method [combining Eqs. (4) and (16)].

which is plotted as the solid curve in Fig. 8. The depth of the minimum of the potential $(h=0)$ was derived by Eisenriegler[36] and reads

$$\frac{W_s(0)}{n_b kT}=-4\pi R R_g^2\ln(2) \quad \text{or} \quad \frac{W_s(0)}{kT}=-3\phi_p\left(\frac{R}{R_g}\right)\ln(2). \tag{17}$$

Here, ϕ_p is the relative polymer concentration which equals $4\pi n_b R_g^3/3$ and is defined such that it is unity at the overlap concentration. From our numerical calculations using Eq. (15) we find $W_s(0)/kT=-227\phi_p$ for $R/R_g=100$, which can be compared with $W_s(0)/kT=-208\phi_p$, as follows from Eq. (17). We can thus conclude that the minimum of the interaction potential from our numerical integration agrees with the Derjaguin approximation to Eq. (4) within 10%. In comparison with the result of the product function, we observe (see Fig. 8) that the range of Eq. (16) is somewhat smaller than our product function approximation. In Fig. 9 we plotted the results from the product functions for $R/R_g=10$, 3, 1, and 0.3. We observe that the range of attraction becomes smaller with decreasing colloid radius, in agreement with a decreasing depletion layer thickness.

C. Consequences for the colloidal stability

The final aim is to understand the consequences of the depletion interaction for the stability of colloidal suspensions containing nonadsorbing polymer chains. The colloidal stability can be expressed by the second osmotic virial coefficient, which is a measure of the effective excluded volume of the colloids. The second osmotic virial coefficient, B_2, is defined as

$$B_2=2\pi\int_0^\infty r^2[1-\exp(-W(r)/kT)]dr, \tag{18}$$

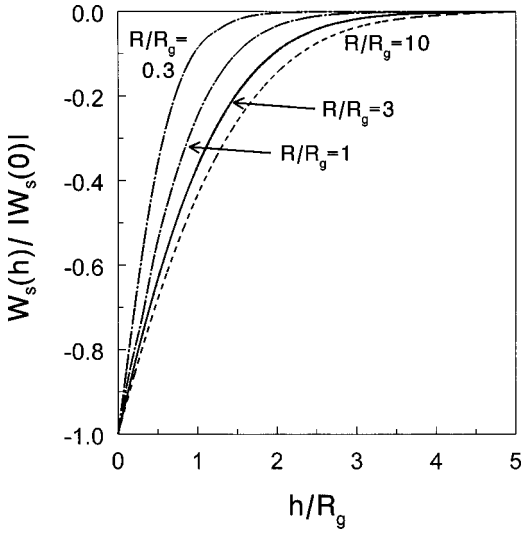

FIG. 9. Interaction potentials as in Fig. 8 between two spheres immersed in an ideal polymer solution for $R/R_g=10$, 3, 1, and 0.3.

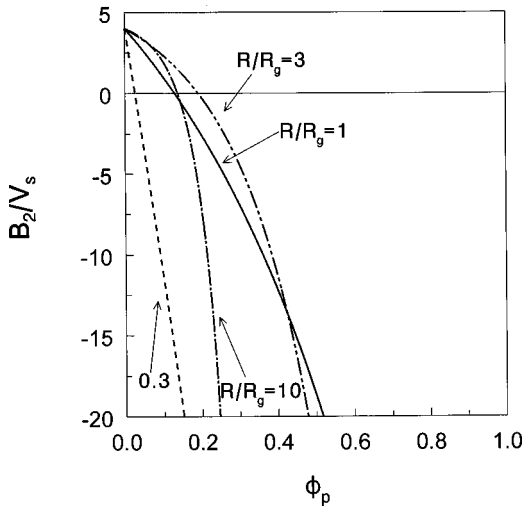

FIG. 11. Second osmotic virial coefficient of hard spheres as a function of the relative polymer concentration as in Fig. 10 for the AO interaction potential.

where r is now the center-to-center distance between the colloidal spheres. For hard spheres B_2 is four times the volume of a particle, and (depletion-induced) attraction will reduce B_2 (at sufficiently high polymer concentrations). When B_2 becomes sufficiently negative a colloidal suspension becomes unstable.[47]

In Fig. 10 we plotted B_2 as a function of the relative polymer concentration for four colloid–polymer size ratios. We see that the depletion interaction becomes ineffective when the polymers become larger than the colloids; B_2 becomes sufficiently negative only when the polymer concentration is close to the overlap concentration. For $R=0.3R_g$ the interaction is ineffective to such a degree that B_2 is always positive in the dilute regime. This explains why rather high polymer concentrations are required to induce phase separation in systems with a relatively large polymer–colloid size ratio.[17–20]

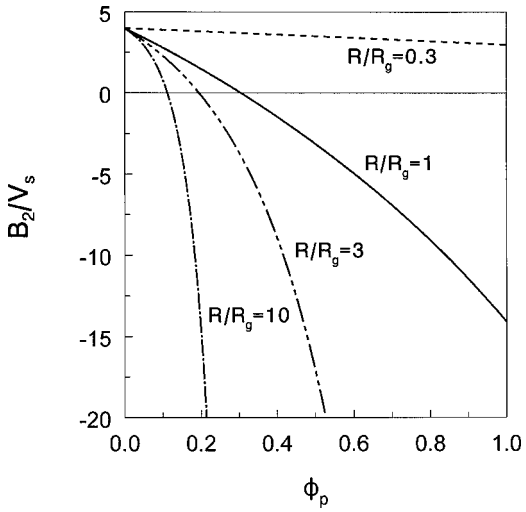

FIG. 10. Second osmotic virial coefficient of hard spheres, normalized with the sphere volume V_s, immersed in a solution of ideal polymer chains as a function of the relative polymer concentration for $R/R_g=10$, 3, 1, and 0.3.

It is illustrative to compare our results with the Asakura–Oosawa (AO) potential between two spheres due to depletion of penetrable hard spheres, as derived by Vrij.[2] We have shown that σ_{PHS} is equal to $4R_g/\sqrt{\pi}$ [see below Eq. (4)]. Consequently, we find for the AO (PHS) potential for two spheres

$$W_s^{\mathrm{AO}}(r)=-\phi_p\left(\frac{R}{R_g}+\frac{2}{\sqrt{\pi}}\right)^3 \times\left[1-\frac{3}{4}\left(\frac{\frac{r}{R_g}}{\frac{R}{R_g}+\frac{2}{\sqrt{\pi}}}\right)+\frac{1}{16}\left(\frac{\frac{r}{R_g}}{\frac{R}{R_g}+\frac{2}{\sqrt{\pi}}}\right)^3\right]. \tag{19}$$

Insertion of this potential into Eq. (18) yields the results plotted in Fig. 11. It is clear that for $R/R_g=10$ and 3 the results for the second osmotic virial coefficient with the AO potential are quite comparable with those obtained with the product function. However, for $R/R_g=1$, and especially for $R/R_g=0.3$, the deviation is quite significant. The PHS approach predicts that phase separation would occur at very low polymer concentrations for spheres smaller than the polymer coils. This shows that a PHS approach is a reasonable approximation only as long as $R/R_g>1$.

IV. CONCLUSIONS

Calculations of the interaction potential between two plates immersed in an ideal polymer solution showed that the interactions could be described in terms of the product function of the single plates only. The results are consistent with computer simulations. Therefore, we proposed that the depletion layer profile around an individual sphere could also be used to describe the interactions between two spheres. The approximated profiles near two spheres also agree with computer simulations. A calculation of the (negative) ad-

sorption around two spheres in a very dilute polymer solution containing ideal chains is shown to be in reasonable agreement with the Derjaguin approximation of the exact result. With increasing polymer–colloid size ratio, the relative range of the interaction decreases. The polymer concentration dependence of the second osmotic virial coefficient shows that the depletion interaction becomes less effective for $R > R_g$ with increasing polymer–colloid size ratio.

ACKNOWLEDGMENTS

The NWO-Unilever program financially supported this work. We would like to thank W. J. Briels, J. K. G. Dhont, G. J. Vroege, P. van der Schoot, and R. Wensink for their help and useful discussions. We thank Dr. T. Taniguchi, Department of Computational Science & Engineering, Nagoya University, Japan, for supplying his M.Sc. thesis.

[1] S. Asakura and F. Oosawa, J. Chem. Phys. **22**, 1255 (1954).
[2] A. Vrij, Pure Appl. Chem. **48**, 471 (1976).
[3] J. F. Joanny, L. Leibler, and P. G. De Gennes, J. Polym. Sci. Pol. Phys. **17**, 1073 (1979).
[4] O. Li-In, B. Vincent, and F. A. Waite, ACS Symp. Ser. **9**, 165 (1975).
[5] B. Vincent, P. F. Luckham, and F. A. Waite, J. Colloid Interface Sci. **73**, 508 (1980).
[6] H. De Hek, and A. Vrij, J. Colloid Interface Sci. **84**, 409 (1981).
[7] A. P. Gast, C. K. Hall, and W. B. Russel, J. Colloid Interface Sci. **96**, 251 (1983).
[8] H. N. W. Lekkerkerker, W. C. K. Poon, P. N. Pusey, A. Stroobants, and P. B. Warren, Europhys. Lett. **20**, 559 (1992).
[9] W. C. K. Poon, Curr. Opin. Colloid Interface Sci. **3**, 593 (1998).
[10] E. J. Meijer and D. Frenkel, J. Chem. Phys. **100**, 6873 (1994).
[11] M. Dijkstra, J. M. Brader, and R. Evans, J. Phys.: Condens. Matter **11**, 10079 (1999).
[12] X. L. Chu, A. D. Nikolov, and D. T. Wasan, Langmuir **12**, 5004 (1996).
[13] P. B. Warren, Langmuir **13**, 4588 (1997).
[14] M. Piech and J. Y. Walz, J. Colloid Interface Sci. **225**, 134 (2000).
[15] A. Milling and S. Biggs, J. Colloid Interface Sci. **170**, 604 (1995).
[16] S. M. Ilett, A. Orrock, W. C. K. Poon, and P. N. Pusey, Phys. Rev. E **51**, 1344 (1995).
[17] M. A. Faers and P. F. Luckham, Langmuir **15**, 2922 (1997).
[18] E. H. A. De Hoog and H. N. W. Lekkerkerker, J. Phys. Chem. B **103**, 5274 (1999).
[19] I. Bodnár, J. K. G. Dhont, and H. N. W. Lekkerkerker, J. Phys. Chem. **100**, 19614 (1996).
[20] I. Bodnár and W. D. Oosterbaan, J. Chem. Phys. **106**, 7777 (1997).
[21] P. G. De Gennes, C.R. Acad. Sci. B **288**, 359 (1979).
[22] E. Eisenriegler, A. Hanke, and S. Dietrich, Phys. Rev. E **54**, 1134 (1996).
[23] A. Hanke, E. Eisenriegler, and S. Dietrich, Phys. Rev. E **59**, 6853 (1999).
[24] E. Eisenriegler, J. Phys.: Condens. Matter **12**, A227 (2000).
[25] T. Odijk, Macromolecules **29**, 1842 (1996).
[26] T. Odijk, Physica A **278**, 347 (2000).
[27] P. van der Schoot, Macromolecules **31**, 4635 (1998).
[28] A. M. Kulkarni, A. P. Chatterjee, K. S. Schweizer, and C. F. Zukoski, Phys. Rev. Lett. **83**, 4554 (1999).
[29] V. Ya. Grinberg, and V. B. Tolstoguzov, Food Hydrocolloids **11**, 145 (1997).
[30] A. Syrbe, W. J. Bauer, and H. Klostermeyer, Int. Dairy J. **8**, 179 (1998).
[31] R. Tuinier and C. G. de Kruif, J. Chem. Phys. **110**, 9296 (1999).
[32] R. Tuinier, J. K. G. Dhont, and C. G. de Kruif, Langmuir **16**, 1497 (2000).
[33] D. G. Hall, J. Chem. Soc., Faraday Trans. 1 **68**, 2169 (1972).
[34] S. G. Ash, D. H. Everett, and C. Radke, J. Chem. Soc., Faraday Trans. 1 **69**, 1256 (1973).
[35] R. Evans, B. Marini, and U. Marconi, J. Chem. Phys. **86**, 7138 (1987).
[36] E. Eisenriegler, Phys. Rev. E **55**, 3116 (1997).
[37] Y. Mao, P. Bladon, H. N. W. Lekkerkerker, and M. E. Cates, Mol. Phys. **92**, 151 (1997).
[38] S. F. Edwards and K. F. Freed, J. Phys. A **2**, 145 (1969).
[39] P. G. De Gennes, *Scaling Concepts in Polymer Physics* (Cornell University Press, Ithaca, 1979).
[40] M. Doi and S. F. Edwards, *The Theory of Polymer Dynamics* (Clarendon Oxford, 1986).
[41] A. Y. Grosberg and A. R. Khoklov, *Statistical Mechanics of Macromolecules* (AIP, New York, 1994).
[42] E. Eisenriegler, J. Chem. Phys. **79**, 1052 (1983).
[43] C. M. Marques and J. F. Joanny, Macromolecules **23**, 268 (1990).
[44] R. I. Feigin and D. H. Napper, J. Colloid Interface Sci. **71**, 117 (1979).
[45] T. Taniguchi, T. Kawakatsu, and K. Kawasaki, *Slow Dynamics in Condensed Matter* AIP Series, edited by K. Kawasaki, **256**, 503 (1992).
[46] B. V. Deryaguin, Kolloid-Z. **69**, 155 (1934).
[47] G. A. Vliegenthart and H. N. W. Lekkerkerker, J. Chem. Phys. **112**, 5364 (2000).